Available online at www.sciencedirect.com
ScienceDirect
Journal of Chromatography A, 1173 (2007) 88–97
JOURNAL OF CHROMATOGRAPHY A
www.elsevier.com/locate/chroma

Liquid chromatography–atmospheric pressure photoionization-mass spectrometry analysis of triacylglycerol lipids—Effects of mobile phases on sensitivity

Sheng-Suan Cai [a,*], Luke Chandler Short [a], Jack A. Syage [a], Michael Potvin [b], Jonathan M. Curtis [b,c]

[a] *Syagen Technology, Inc., 1411 Warner Avenue, Tustin, CA 92780, USA*
[b] *Ocean Nutrition Canada, 101 Research Drive, Dartmouth, Nova Scotia B2Y 4T6, Canada*
[c] *Department of Agricultural, Food and Nutritional Science, University of Alberta, Edmonton, Alberta T6G 2P5, Canada*

Received 5 July 2007; received in revised form 26 September 2007; accepted 3 October 2007
Available online 10 October 2007

Abstract

In this work, we evaluate the performance of liquid chromatography–atmospheric pressure photoionization-mass spectrometry (LC–APPI-MS) for non-aqueous reversed phase analysis of six triacylglycerol model compounds using six binary mobile phases including MeOH/iPrOH, MeOH/$CHCl_3$, MeOH/CH_2Cl_2, CH_3CN/iPrOH, CH_3CN/$CHCl_3$, and CH_3CN/CH_2Cl_2. All mobile phases give comparably good separation performance on a Gemini C_{18} column with carefully adjusted gradient elution programs. APPI sensitivity varies from one mobile phase to the other without dopants; however use of dopants brings sensitivity to comparable levels for all mobile phases. MeOH/iPrOH offers high sensitivity without dopants due to self-doping effect and dopants are not necessary for this mobile phase. Dopants enhance analyte sensitivity to a varying degree for each of the mobile phases tested. Photo-induced chemical ionization (PCI) of solvent may play a significant role in achieving high sensitivity. Two critical parameters affecting sensitivity are photoabsorption cross-sections and ionization potentials of mobile phase solvents. How these mobile phase solvents affect APPI sensitivity and their dependency on dopant use are discussed. All six mobile phases offer comparable overall limits of detection for the analytes tested. These results indicate that LC–APPI-MS is a successful tool for neutral lipid analysis, giving high sensitivity with a variety of non-aqueous mobile phases.

Keywords: Atmospheric pressure photoionization; APPI; Mass spectrometry; LC/MS; Lipids; Triacylglycerols; Non-aqueous reversed phase separation

1. Introduction

Triacylglycerols (TAGs) are the major components of naturally occurring fats and oils from animal and vegetable sources. Structurally, TAGs consist of three fatty acids esterified to a glycerol molecule (Fig. 1). Since TAGs are ubiquitous in plants and animals adapted to a wide range of environments and functions, they occur as complex mixtures made up of saturated, monounsaturated and polyunsaturated fatty acyl chains with a wide variety of chain lengths [1]. The widespread occurrence of TAGs along with their nutritional [2] and industrial importance have resulted in considerable efforts in developing analytical methods [3] to determine not only TAG fatty acid compositions but also the '*sn*' values (i.e., stereochemical numbering), used to classify the spatial positions of fatty acyl groups.

Due to the complexity of TAG mixtures, direct LC analysis of TAGs cannot usually be achieved without the coupling LC to a mass spectrometer (MS). The LC/MS interfaces most commonly used employs atmospheric pressure ionization (API) techniques, such as electrospray ionization (ESI) and atmospheric pressure chemical ionization (APCI) [4]. Atmospheric pressure photoionization (APPI) is an alternative technique, demonstrated in previous research [5,6] to detect TAGs with better overall performance than either ESI or APCI. The previous results indicate that APPI and APCI offer comparable linear dynamic ranges (i.e., 4 to 5 decades) and further indicate that APPI is approximately two to four times more sensitive than APCI. In addition, APPI is much more sensitive than ESI when mobile phases without modifiers are used. Use of mobile phase additives (e.g., ammonium

* Corresponding author. Tel.: +1 714 258 4400x26; fax: +1 714 258 4404.
E-mail address: vcai@syagen.com (S.-S. Cai).

0021-9673/$ – see front matter © 2007 Elsevier B.V. All rights reserved.
doi:10.1016/j.chroma.2007.10.008

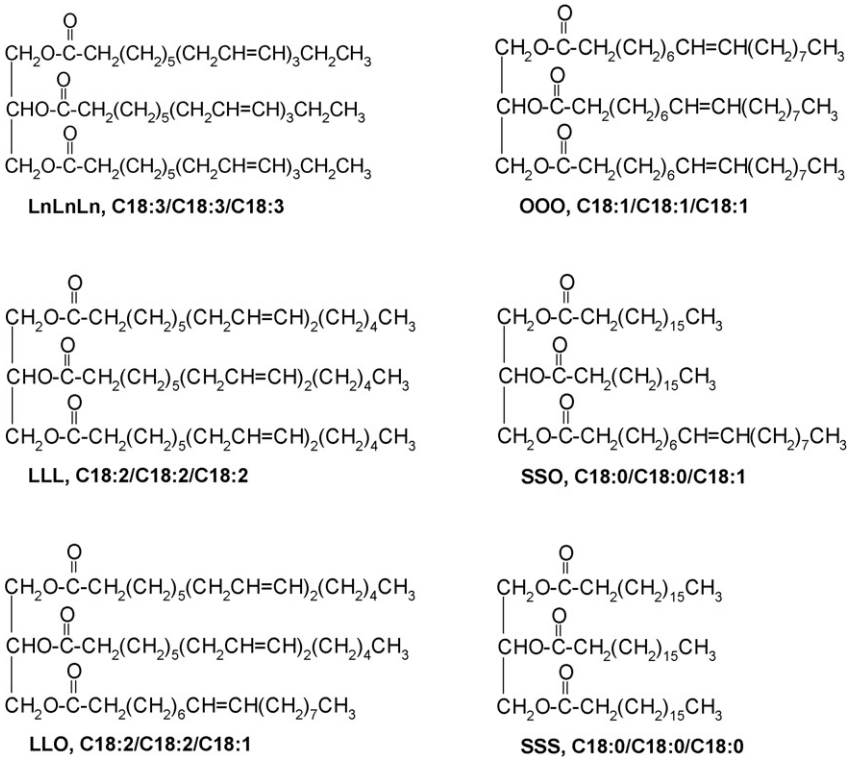

Fig. 1. Chemical structure of TAG analytes.

formate) dramatically enhances the sensitivity of ESI, but with a sharply reduced linear range and an increase in the complexity of the resulting mass spectra. The effects of various mobile phase compositions on the APPI sensitivity of lipids have also been previously investigated [6]. However, most of the previous work was performed with flow-injection analysis (FIA) without any chromatographic separation. The performance of TAG with LC separation combined with an APPI-MS has not been extensively evaluated before and is the subject of this work.

In previous work, APPI sensitivity was shown to be highly dependent on mobile phase composition [6]. The chemical and physical properties of the mobile phase solvents affect APPI sensitivity in several aspects including volatility [6], proton affinity [7], gas phase acidity [8] photoabsorption cross-section (i.e., degree of photoabsorption) [9] and ionization potential (IP) [9]. In particular, the photoabsorption cross-section and ionization potential (IP) of solvents are believed to be two major parameters affecting APPI sensitivity. In the present case, photoionization is achieved using a lamp filled with Kr gas, producing vacuum UV (VUV) light at energies of 10.0 eV and 10.6 eV via radiofrequency discharge. Due to the limited photon flux from the Kr lamp and the abundance of mobile phase present in the APPI source, the photoabsorption of the mobile phase solvents plays a significant role on the ionization efficiency of analyte molecules. The resulting probability of an analyte molecule being directly photoionized is relatively small under atmospheric pressure [9]. Whether solvent photoabsorption has a positive or negative effect on sensitivity ultimately depends on whether the solvent is readily ionizable or not. Neither mobile phase solvents nor analytes with IPs higher than photon energies (i.e., 10.0 eV and 10.6 eV from a Kr lamp) can be *directly* photoionized. APPI-initiated APCI (also termed photo-induced chemical ionization, or PCI) [10] can play a major role in achieving high APPI sensitivity [9]. In other words, solvent and dopant molecules (if present) are photoionized, and then subsequently undergo ion-molecule reactions resulting in analyte ions.

In this work, a mixture of six TAG model compounds was separated by non-aqueous reversed phase chromatography using a C_{18} column. Six binary mobile phases are investigated including MeOH/iPrOH, MeOH/$CHCl_3$, MeOH/CH_2Cl_2, CH_3CN/iPrOH, CH_3CN/$CHCl_3$ and CH_3CN/CH_2Cl_2. Experiments were performed with and without dopants, using two different APPI source designs. We discuss how each of the mobile phases affects APPI sensitivity based upon solvent properties such as photoabsorption and IP. The results presented here demonstrate that LC–APPI-MS is a powerful technique for neutral lipid analysis, providing a high level of sensitivity with a wide variety of non-aqueous mobile phases. As an illustration of the use of non-aqueous reversed phase LC–APPI-MS, the method is then applied to the highly complex mixture of TAGs present in natural oil from fish of the genus *Sarda* (bonito), demonstrating the high level of structural specificity that can be readily achieved by this type of analysis.

2. Experimental

2.1. Chemicals and reagents

TAG model compounds include: tristearin (SSS), 1,2-distearoyl-3-oleoyl-*rac*-glycerol (SSO), triolein (OOO), 1,2-

Table 1
Effects of ECN and cone voltages on major ions of TAG analytes[a]

Name	Symbol	ECN	TAG type	Major ion *m/z*	Optimum cone (V)	Relative peak intensity at optimum cone voltage
Tristearin	SSS	54	C18:0/C18:0/C18:0	607.6 $[MH–C18:0]^+$ 913.8 $[M+Na]^+$	45 65	$[MH–C18:0]^+ > [M+Na]^+$
1,2-Distearoyl-3-oleoyl-*rac*-glycerol	SSO	52	C18:0/C18:0/C18:1 [*cis*]-9	605.7 $[MH–C18:0]^+$ 607.6 $[MH–C18:1]^+$ 890 $[MH]^+$ 911.7 $[M+Na]^+$	45 45 30 65	$[MH–C18:1]^+ > [MH–C18:0]^+ > [M+Na]^+ > [MH]^+$
Triolein	OOO	48	C18:1/C18:1/C18:1 all [*cis*]-9	603.6 $[MH–C18:1]^+$ 885.8 $[MH]^+$ 907.8 $[M+Na]^+$	45 35 65	$[MH–18:1]^+ > [MH]^+ > [M+Na]^+$
1,2-Dilinoleoyl-3-oleoyl-*rac*-glycerol	LLO	44	C18:2 [*cis*]-9,12/C18:2 [*cis*]-9,12/C18:1 [*cis*]-9	599.6 $[MH–C18:1]^+$ 601.6 $[MH–C18:2]^+$ 881.8 $[MH]^+$ 903.7 $[M+Na]^+$	45 45 45 65	$[MH]^+ > [MH–C18:2]^+ > [MH–C18:1]^+ > [M+Na]^+$
Trilinolein	LLL	42	C18:2/C18:2/C18:2 all [*cis*,*cis*]-9,1 2	599.6 $[MH–C18:2]^+$ 879 7 $[MH]^+$ 901.7 $[M+Na]^+$	45 45 60	$[MH]^+ > [MH–C18:2]^+ > [M+Na]^+$
Trilinolenin	LnLnLn	36	C18:3/C18:3/C18:3 all[*cis*,*cis*,*cis*]-9, 12, 15	595.5 $[MH–C18:3]^+$ 873 7 $[MH]^+$ 896.7 $[M+Na]^+$	50 45 60	$[MH]^+ > [MH–C18:3]^+ > [M+Na]^+$

[a] TAG: triacylglycerol; ECN: equivalent carbon number. $[MH–C18:0]^+$, $[MH–C18:1]^+$, $[MH–C18:2]^+$ and $[MH–C18:3]^+$: denoting protonated molecules with loss of C18:0, C18:1, C18:2 and C18:3 fatty acid moiety, respectively. Near-optimal cone voltage range is obtained from MassLynx tune page by infusion analysis of 1 ppm analyte in iPrOH at iPrOH mobile phase flow rate of 50 μL/min. The cone voltage is further optimized by acquiring major ions in SIM mode at voltage interval of 5 V each within the near-optimal range obtained from the tune page.

dilinoleoyl-3-oleoyl-*rac*-glycerol (LLO), trilinolein (LLL) and trilinolenin (LnLnLn). The compounds SSS, SSO, OOO and LLO were purchased from Sigma–Aldrich (St. Louis, MO, USA). Both LLL and LnLnLn were purchased from Nu-Chek Prep (Elysian, MN, USA). All lipid standards are of at least 98% purity. The chemical structures of TAG analytes are presented in Fig. 1. The TAG type and the degree of unsaturation (i.e., equivalent carbon number or ECN) of these chemicals are summarized in Table 1.

Acetonitrile (CH_3CN), HPLC grade, 99.9% purity, was purchased from Acros Organics (NJ, USA). Methanol (MeOH), B&J ACS/HPLC certified solvent, was purchased from Burdick & Jackson (Muskegon, MI, USA). Isopropyl alcohol (iPrOH), residue grade, was purchased from EM Science (Gibbstown, NJ, USA). Chloroform ($CHCl_3$) and dichloromethane (CH_2Cl_2), Chromasolv Plus, for HPLC, 99.9%, were both purchased from Sigma–Aldrich. Acetone and toluene, Chromasolv, for HPLC (≥99.9%), were both purchased from Sigma–Aldrich.

Semi-refined bonito oil (fish of the genus *Sarda*) was produced by Ocean Nutrition Canada (Dartmouth, Nova Scotia, Canada).

2.2. Instruments

Waters Micromass ZQ LC–MS equipped with APCI and ESI sources and the MassLynx v4.0 data processing software (Waters, Milford, MA, USA) was used for this work except where stated. The instrument was equipped with Waters 2795 Separations Module and PhotoMate APPI source (Syagen Technology, CA, USA). A Phenomenex Gemini C_{18} column (150 mm × 2 mm, 5 μm) was used for the separation of standards. Other experiments used a Waters Micromass Q-Tof-1 mass spectrometer with a Syagen PhotoMate APPI source (cone voltage 40–45 V, source block temperature 140 °C and desolvation temperature of 450 °C) and an Agilent 1100 LC. A Waters RX-C_{18} column (150 mm × 2.1 mm, 5 μm) was used for the fish oil analysis.

2.3. Preparation of standards

Stock solutions of individual standards were prepared in $CHCl_3$ at a concentration of 10.0 μg/μL each for SSS, OOO, LLL and LnLnLn, and at 1.0 μg/μL and 2.5 μg/μL for SSO and LLO, respectively. Working standards of individual components and a standard mixture were prepared from stock solutions by a series dilution method using iPrOH.

2.4. Optimization of cone voltage

The proper selection of analyte cation and its corresponding cone voltage are key factors in optimum sensitivity of APPI-MS [6,9]. A general set of parameters was used to perform the TAG full scan analysis (repeller = 0.7 kV; APCI probe = 450 °C; cone = 40 V; desolvation gas = 400 L/h; extractor = 3 V; RF lens = 0.2 V; source = 150 °C). Near-optimal cone

voltage ranges were obtained using the MassLynx tune page for each major ion by infusion analysis of 1 ppm of individual analyte standard with an iPrOH mobile phase flow rate of 50 μL/min. Cone voltage were further optimized by acquiring each major ion in selected ion monitoring (SIM) mode at voltage interval of 5 V each within the near-optimal range obtained from the tune page. The optimal cone voltages for major ions are presented in Table 1.

3. Results and discussion

3.1. APPI full scan mass spectra of TAGs

The APPI and APCI full scan mass spectra of a fatty acid methyl ester and acylglycerols (monoacylglycerol, diacylglycerol and triacylglycerol) were compared in a previous work [5], where it was demonstrated that both ionization techniques generate similar mass spectra of these compounds. For example, the most intense ion observed with both APPI and APCI of trielaidin (*t*C18:1/*t*C18:1/*t*C18:1, MW = 885.4 g/mol) is the fragment ion $[M+H–282]^+$, resulting from the loss of one molecule of elaidic acid. The formation of these $[M–RCOO]^+$ fragment ions are present in the APCI mass spectra of triglycerides, and their intensities can be used to infer the fatty acyl group on the *sn*-2 position [11]. We present in Fig. 2 the APPI mass spectra of six TAGs with different degrees of unsaturation. Full scan mass spectra were obtained by flow-injection of 10 ng of each analyte in iPrOH, with an iPrOH mobile phase flow rate of 50 μL/min. A constant, near-optimal, cone voltage of 40 V was used to generate all APPI mass spectra.

Tristearin (SSS, C18:0/C18:0/C18:0, MW = 890.7 g/mol) gave a major fragment ion of *m/z* 607.6, corresponding to $[M–C_{17}H_{35}COO]^+$, a neutral loss of 284 (stearic acid) from the protonated molecule. A sodium adduct ion $[M+Na]^+$ at *m/z* 913.9 was also observed with low intensity, but virtually none of the protonated parent ion was seen. The absence of protonated molecules for fully saturated TAGs has also been noted previously using APCI [4,11].

1,2-Distearoyl-3-oleoyl-*rac*-glycerol (SSO, C18:0/C18:0/C18:1, MW = 888.7 g/mol) resulted in two major fragment ions, *m/z* 607.6 and *m/z* 605.7, with m/z 607.6 slightly higher in intensity. The fragment ion at *m/z* 607.6 $[M–C_{17}H_{33}COO]^+$ arose from a neutral loss of 282 (i.e., oleic acid) from the protonated molecule whereas *m/z* 605.7 is $[M–C_{17}H_{35}COO]^+$, corresponding to a neutral loss of 284 (stearic acid) from the protonated parent compound. The similar intensity of these two fragment ions confirms the substitution as SSO rather than SOS, where a much lower intensity for loss of oleic acid from the *sn*-2 position would be expected, as seen with the ions generated using APCI [11]. A low intensity sodium adduct ion at *m/z* 911.9 was also observed.

Triolein (OOO, C18:1/C18:1/C18:1, MW = 884.7 g/mol) gave the fragment ion *m/z* 603.6 $[M–C_{17}H_{33}COO]^+$ as the base peak and *m/z* 885.9 $[M+H]^+$, and *m/z* 907.8 $[M+Na]^+$ with much lower intensity. Under different source conditions an ion at *m/z* 902.8 $[M+NH_4]^+$ has been observed in place of the $[M+Na]^+$ peak.

1,2-Dilinoleoyl-3-oleoyl-*rac*-glycerol (LLO, C18:2/C18:2/C18:1, MW = 880.7 g/mol) also gave two major fragment ions at *m/z* 601.6 (loss of linoleic acid, L, from the protonated molecule) and *m/z* 599.6 (loss of oleic acid, O, from the protonated molecule). The *m/z* 601.6 signal intensity is slightly higher than that of *m/z* 599.6 due to loss of L from either of two positions though the *sn*-2 position is much less favored. The

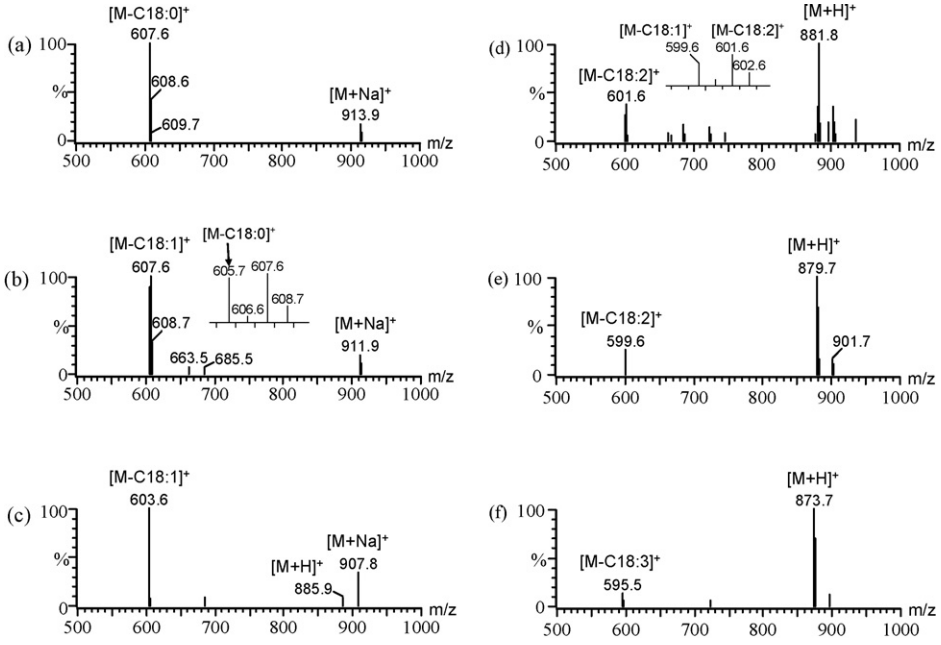

Fig. 2. APPI + full scan mass spectra of TAGs. Injection amount: 10 ng each. (a) SSS, C18:0/C18:0/C18:0; (b) SSO, C18:0/C18:0/C18:1; (c) OOO, C18:1/C18:1/C18:1; (d) LLO, C18:2/C18:2/C18:1; (e) LLL, C18:2/C18:2/C18:2; (f) LnLnLn, C18:3/C18:3/C18:3. As the degree of unsaturation increases, the intensity of protonated molecules increases.

protonated molecule *m/z* 881.8 is the most abundant ion in the mass spectrum of LLO.

Trilinolein (LLL, C18:2/C18:2/C18:2, MW = 878.7 g/mol) gave a protonated parent ion peak of *m/z* 879.7, and a major fragment ion of *m/z* 599.6, corresponding to a neutral loss of 280 (linoleic acid) from the protonated parent ion. Similarly, trilinolenin (LnLnLn, C18:3/C18:3/C18:3, MW = 872.7 g/mol) gave a base peak protonated molecule of *m/z* 873.7, and a major fragment ion of *m/z* 595.5, corresponding to a neutral loss of 278 (linolenic acid) from the protonated molecule.

Overall, the results shown in Fig. 2 indicate that $[M+H]^+$ and the fragment ions $[M–RCOO]^+$ were the dominant ions in the positive ion APPI mass spectra of all six TAGs tested. It is observed in Fig. 2 that the relative intensity of the protonated TAG molecule increases as the number of double bonds present in the TAG rises. One way of illustrating this is by use of the equivalent carbon number (ECN) [12] for these TAGs. Since all of the TAGs studied (Fig. 2 and Table 1) contain only 18 carbon acyl chains, the ECN's only reflect the degree of unsaturation. Here we see that as the ECN decreases (i.e., degree of unsaturation increases), intensities of the protonated parent ions increase. This is likely a result of the increase in basicity of polyunsaturated hydrocarbons (specifically the double bonds) over their equivalent saturated counterparts. In addition, by comparing the ion intensity ratio of two fragment ions generated from the same TAG compound such as SSO or LLO (each of which contains only two types of fatty acyl groups), bond cleavage slightly favors the fatty acid moiety with a higher degree of unsaturation when the hetero-C18 fatty acid moieties are located at the *sn*-1 or *sn*-3 position of glycerol backbone. However, a larger set of TAGs would need to be studied to conclusively demonstrate this rule. In summary, the TAG APPI mass spectra look very similar to those of APCI reported by previous researchers [4,11].

3.2. Establishments of mobile phases for NA-RP-LC separations of TAGs

TAG LC separations are usually achieved by either normal phase high performance liquid chromatography (NP-HPLC) using silica columns [13], by silver ion-HPLC or by C_{18}-HPLC under non-aqueous reversed phase (NA-RP) HPLC conditions. However, much of the reported TAG analysis has been performed using NA-RP-LC separations due to the higher resolving power achievable with complex mixtures of TAGs [12]. Aqueous reversed phase LC separations of TAGs are difficult to achieve due to poor solubility of TAGs in water and polar solvents. Often, NA-RP HPLC separations employ binary mobile phase systems with gradient elution, from low to high solvent-strength. In this work, the commonly used reversed phase solvents MeOH and CH_3CN (very poor solvents for TAGs) are selected as weak solvent-strength mobile phase components (i.e., mobile phase A). The solvents iPrOH, $CHCl_3$ and CH_2Cl_2 offer good solubility for TAG analytes and are therefore selected as high solvent-strength mobile phase components (i.e., mobile phase B). With these solvent components, six binary mobile phase systems were selected for evaluation of LC–APPI-MS sensitivity and performance: MeOH/iPrOH, MeOH/$CHCl_3$, MeOH/CH_2Cl_2, CH_3CN/iPrOH, CH_3CN/$CHCl_3$ and CH_3CN/CH_2Cl_2. Some of these mobile phases have been used previously to chromatographically separate many TAG analytes in various sample matrixes. As an example the mixture CH_3CN/iPrOH was used as a binary solvent system for separation of TAGs in donkey milk and lipidic matrixes [12,14–16]. The mobile phases CH_3CN/$CHCl_3$ and CH_3CN/CH_2Cl_2 are frequently used for TAG analysis [4,12].

3.3. On-column analysis of TAGs

LC separations were achieved by gradient elution using a 150 mm × 2.0 mm, 5 μm, Phenomenex Gemini C_{18} reversed phase column with the above mentioned six binary mobile phases at a flow rate of 200 μL/min. 10 ng of each TAG analyte was injected on-column from a mixture of TAG standards containing 1 ng/μL of each analyte. Gradient elution was from 90% of the weaker solvent (MeOH or CH_3CN) to 40–70% of the stronger solvent (iPrOH, CH_2Cl_2 or $CHCl_3$). In order to compare the sensitivity achieved using the mobile phases tested, the gradient elution programs were adjusted to achieve comparable chromatographic separations for each case. The LC/MS chromatograms and exact gradients used are shown in Fig. 3. All six mobile phases result in comparable column separation performances for all six-model compounds, given the appropriate gradient elution. The analyte elution order follows the ECNs of the six analytes for all six mobile phases, i.e., increasing retention time in the order LnLnLn < LLL < LLO < OOO < SSO < SSS. This is consistent with the literature reports [12].

We find that MeOH- and iPrOH-containing mobile phases resulted in higher column backpressure than mobile phases containing CH_3CN, $CHCl_3$ or CH_2Cl_2. In fact, the MeOH/iPrOH solvent system gave the highest column backpressure among all tested mobile phases, producing the broadest signal peaks (Fig. 3). In contrast, $CHCl_3$-containing mobile phases resulted in the narrowest peaks and shortest retention times without sacrificing resolution. However, the mobile phase CH_3CN/iPrOH was preferred in general because it generates lower column backpressure and narrower peak widths than MeOH/iPrOH. Further, it avoids the environmental hazards of chlorinated solvents including unpleasant odors during desolvation and vaporization, and was found suitable for stable LC–APPI-MS operation during overnight runs.

Acetone and toluene were evaluated as dopants, resulting in a sensitivity enhancement for APPI. Dopants were added by post-column addition using a syringe pump and a Mixing Tee at a flow rate of 40 μL/min, determined from past experience, and used without further optimization. The effects of these mobile phases on APPI sensitivity of analytes and their dependency on the use of dopants are discussed in the next section.

3.4. Effects of solvents on APPI sensitivity

APPI can occur either *via* direct photoionization of the analyte or *via* APCI processes following photoionization of the

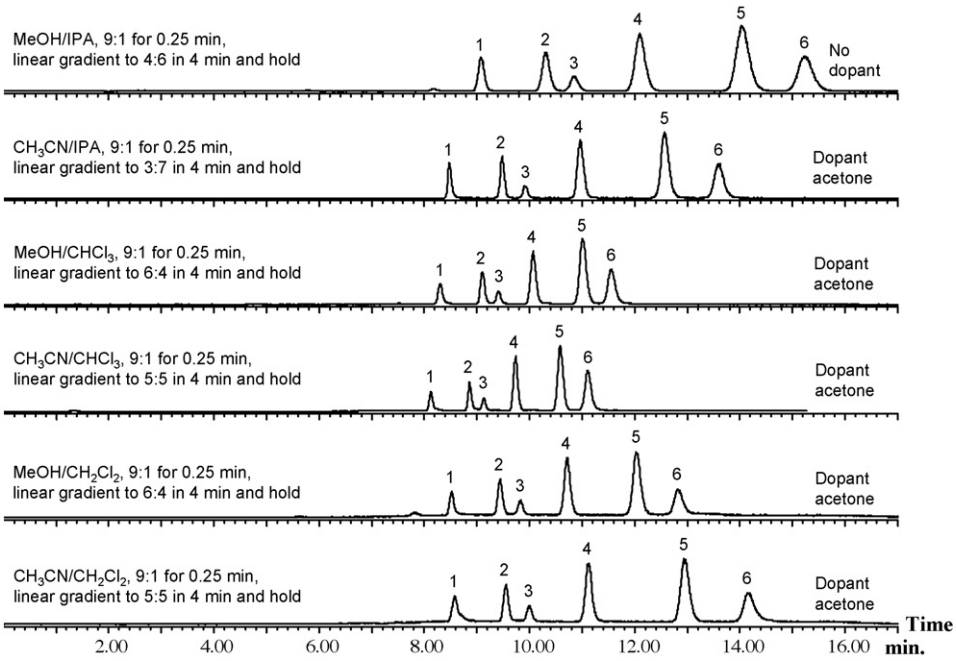

Fig. 3. Non-aqueous reversed phase separation of TAG lipids. Analyte ID: (1) LnLnLn, (2) LLL, (3) LLO, (4) OOO, (5) SSO, (6) SSS. Waters ZQ LC–APPI-MS. 150 mm × 2 mm, 5 μm, Gemini C18 column. Mobile phase flow rate 0.2 mL/min, dopant flow rate 0.04 mL/min, 10 ng each.

solvent vapor or dopant (i.e., ion-molecule reactions) [9,17]. Hence, major factors affecting sensitivity include the ionization potentials (IPs) of solvent and analyte species and the relative proton affinities of solvent cluster ions and analytes. Another factor affecting the abundance of analyte ions is the attenuation of the light source caused by the photoabsorption of the solvent. The dependence of photoabsorption on solvent type, solvent flow and photon energy has been described recently [9]. With the 10.0 eV and 10.6 eV photon energies emitted from a Kr VUV lamp used here, the photoabsorption cross-sections are significant for all of the mobile phases studied. These range from $\sim 15 \times 10^{-18}$ cm^2 for MeOH to $\sim 130 \times 10^{-18}$ cm^2 for CH_2Cl_2, with iPrOH and $CHCl_3$ at intermediate values in the range $36–39 \times 10^{-18}$ cm^2 [9]. The solvent molecule CH_3CN shows an absorption maximum at ~10.6 eV, and hence the measured cross-section at 10.6 eV (120×10^{-18} cm^2) is much higher than at 10.0 eV (24×10^{-18} cm^2). The data presented in Table 2 indicates that without dopants the mobile phase with the highest photoabsorption cross-section (CH_3CN/CH_2Cl_2) results in the lowest triglyceride APPI response (protonated molecule or fragment ion). Conversely, the mobile phase with one of the lowest photoabsorption cross-sections (MeOH/iPrOH) gives the highest triglyceride APPI response. This could be explained by the extent of attenuation of the light source due to non-ionizing photoabsorption. However, an explanation of the results for the intermediate mobile phases is less obvious, and it is likely that the APPI mechanism is much more complex, involving a number of factors, as described above.

Since photo-induced chemical ionization (PCI) of the solvent can play a significant role in achieving enhanced APPI sensitivity [9], the ionization potentials of solvent molecules must be considered. In Fig. 4 it is shown that none of the mobile phase solvents used here have IPs below the 10.0 eV Kr line although the ionizable MeOH dimers are known to form (see discussion below). In addition to MeOH dimers, only iPrOH has an IP below the other Kr lamp line, 10.6 eV. To enhance PCI processes, small concentrations of miscible solvent "dopants" possessing low IPs, e.g., acetone (IP = 9.7 eV) or toluene (IP = 8.82 eV), may be added post-column. Ion-molecule reactions of ionizable mobile phase solvents and/or dopants are responsible for the indirect photoionization of analytes.

It can be seen from Fig. 4 that PCI processes are possible without the addition of a dopant to the mobile phases. This is consistent with the results presented in Table 2—all four solvent combinations containing alcohols show significant APPI analyte peak areas, with the highest being the MeOH/iPrOH combination. In contrast, the two mobile phases containing CH_3CN plus either CH_2Cl_2 or $CHCl_3$ give rise to little or no APPI analyte peak area. Table 2 shows that non-

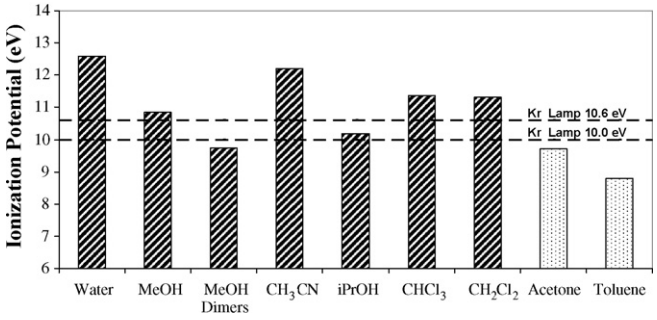

Fig. 4. Ionization potentials of solvents and dopants. The 10.0 eV and 10.6 eV Kr lines are shown as dashed lines.

Table 2
Effects of mobile phase solvents and dopants on peak area of TAG analytes[a]

Mobile phase	Analyte	Acquired ion	Peak area			Average factor enhanced acetone	Average factor enhanced toluene
			No dopant	Dopant acetone	Dopant toluene		
MeOH/iPrOH	LnLnLn	873.7 $[MH]^+$	7.0	5.6	5.0	0.8	0.8
	LLL	879.7 $[MH]^+$	8.9	7.0	7.0		
	LLO	881.8 $[MH]^+$	3.9	2.7	3.1		
MeOH/CH_2Cl_2	LnLnLn	873.7 $[MH]^+$	4.5	5.5	5.6	1.2	1.3
	LLL	879.7 $[MH]^+$	6.1	6.8	7.5		
	LLO	881.8 $[MH]^+$	2.7	3.0	3.7		
CH_3CN/iPrOH	LnLnLn	873.7 $[MH]^+$	1.6	3.2	2.7	1.8	1.8
	LLL	879.7 $[MH]^+$	2.1	4.1	3.9		
	LLO	881.8 $[MH]^+$	1.0	1.5	1.8		
MeOH/$CHCl_3$	LnLnLn	873.7 $[MH]^+$	1.2	6.4	6.0	5.5	6.8
	LLL	879.7 $[MH]^+$	1.4	7.5	9.6		
	LLO	881.8 $[MH]^+$	0.5	3.1	4.5		
CH_3CN/$CHCl_3$	LnLnLn	873.7 $[MH]^+$	0.2	6.2	4.2	39.4	41.1
	LLL	879.7 $[MH]^+$	0.2	7.6	8.5		
	LLO	881.8 $[MH]^+$	0.1	3.4	4.4		
CH_3CN/CH_2Cl_2	LnLnLn	873.7 $[MH]^+$	ND	6.1	4.8		
	LLL	879.7 $[MH]^+$	ND	7.7	7.3		
	LLO	881.8 $[MH]^+$	ND	3.6	3.8		
MeOH/iPrOH	OOO	603.6 $[MH–C18:1]^+$	19.8	16.1	13.7	0.8	0.7
	SSO	605.7 $[MH–C18:0]^+$	16.0	12.3	10.9		
	SSS	607.6 $[MH–C18:0]^+$	19.0	14.9	14.0		
MeOH/CH_2Cl_2	OOO	603.6 $[MH–C18:1]^+$	13.3	15.7	15.3	1.1	1.2
	SSO	605.7 $[MH–C18:0]^+$	10.9	12.0	11.5		
	SSS	607.6 $[MH–C18:0]^+$	10.4	10.7	13.5		
CH_3CN/iPrOH	OOO	603.6 $[MH–C18:1]^+$	5.6	9.4	7.8	1.7	1.5
	SSO	605.7 $[MH–C18:0]^+$	4.4	7.2	6.3		
	SSS	607.6 $[MH–C18:0]^+$	5.4	8.9	8.1		
MeOH/$CHCl_3$	OOO	603.6 $[MH–C18:1]^+$	2.7	16.2	16.9	6.1	6.6
	SSO	605.7 $[MH–C18:0]^+$	2.2	13.8	13.6		
	SSS	607.6 $[MH–C18:0]^+$	2.6	16.1	19.9		
CH_3CN/$CHCl_3$	OOO	603.6 $[MH–C18:1]^+$	3.8	19.4	14.1	6.6	6.2
	SSO	605.7 $[MH–C18:0]^+$	3.0	15.8	10.9		
	SSS	607.6 $[MH–C18:0]^+$	2.4	23.1	27.2		
CH_3CN/CH_2Cl_2	OOO	603.6 $[MH–C18:1]^+$	ND	18.0	10.8		
	SSO	605.7 $[MH–C18:0]^+$	ND	13.8	7.5		
	SSS	607.6 $[MH–C18:0]^+$	ND	16.4	15.8		

[a] Peak area for MeOH/iPrOH without dopant is the average of triplicate analyses. All other peak area is based on a single injection analysis. All peak area is divided by a factor of 1000 for easy visual comparison.

dopant APPI of TAGs yielding the $[M+H]^+$ parent ion in differing solvent mixes results in relative peak area intensities of MeOH/iPrOH > MeOH/CH_2Cl_2 > CH_3CN/iPrOH > MeOH/$CHCl_3$ ≥ CH_3CN/$CHCl_3$ > CH_3CN/CH_2Cl_2. A similar trend was observed for the TAG fragment ions representing $[M–RCOO]^+$, although there is reversal of the order between MeOH/$CHCl_3$ and CH_3CN/$CHCl_3$ for OOO and SSO.

3.5. Effects of dopants on APPI sensitivity

The high APPI peak area for all TAG mass spectra obtained with the MeOH/iPrOH system is not enhanced by post-column addition of acetone or toluene (Table 2). Furthermore, with the MeOH/CH_2Cl_2 mobile phase, dopants only result in a minor enhancement in response for TAGs. This is due to the "self-doping" effects of these two solvent systems, i.e., they are amenable to direct photoionization. Dopants do, however, dramatically enhance the intensity of TAGs for the other mobile phases listed (Table 2). The extent of enhancement follows the reverse trend of TAG peak intensity without dopants (described above). Thus, the greatest signal enhancement using dopants is seen with the CH_3CN/CH_2Cl_2 combination, which also has the highest IPs.

In the cases where solvent monomer IPs is higher than Kr lamp photon energies, solvent clusters can form within the ion source. The MeOH monomer has an IP of 10.85 eV and does not

directly photoionize with light from a Kr lamp. However, within the source there is a significant amount of MeOH dimer formed [9], having a much lower IP of 9.74 eV [18], making photoionization possible. The APPI mass spectrum of MeOH alone shows major ions of $[CH_3OH]H^+$, $[CH_3OH]_2H^+$ and $[CH_3OH]_3H^+$. In this case, protonated MeOH molecules are believed to be formed as a result of collision induced dissociation (CID) products or photo-induced cluster reactions of the MeOH dimer (and to a lesser extent trimer) [9]. Although the direct photoionization of the MeOH dimer yields radical cations, these species are also believed to undergo kinetically driven, rapid H-abstraction reactions [19] as well as cluster formation reactions [9].

In the case of iPrOH, which can be directly ionized by the light from a Kr lamp, the mass spectrum shows major ions of $[iPrOH]H^+$, $[iPrOH]_2H^+$ and $[iPrOH]_3H^+$. These indicate that similar H-atom abstraction and clustering reactions occur for iPrOH as observed for MeOH.

The solvent molecule CH_3CN has an IP above Kr lamp photon energies (Fig. 4) and yet the protonated CH_3CN monomers, dimers and protonated propionitrile (CH_3CH_2CN) ions are present in the APPI CH_3CN mass spectrum. The total intensities of CH_3CN solvent ions are much lower than those for MeOH and CH_2Cl_2. The mechanism of formation of propionitrile ions in the APPI mass spectra of CH_3CN solvent has been discussed [9], and is thought to involve the more facile ionization of CH_3CN dimers, in a manner similar to what is observed for MeOH.

Overall, use of dopants has been found most effective at enhancing sensitivity for solvent systems that cannot be directly ionized as well as those solvents with high photoabsorption cross-sections. Thus, CH_3CN/CH_2Cl_2 and $CH_3CN/CHCl_3$ solvent systems give little or no response for 10 ng injections of all six TAGs without dopants, but comparable sensitivity to other mobile phases when acetone or toluene dopants are used (Table 2).

Both dopants are found to offer comparable overall peak area for a specific analyte regardless of the mobile phases used (Table 2). However, earlier reports have demonstrated that the level of baseline noise in LC–APPI-MS may be greater when toluene is used compared to acetone. This has been previously found with fat-soluble vitamins [17] or the normal phase chiral separation of pharmaceutical drugs [20]. In the present work, this effect was also seen using the Waters Micromass ZQ mass spectrometer, but when a flow-injection experiment was run using a Waters Micromass Q-Tof-1, which has similar source geometry with a mobile phase of CH_3CN/iPrOH, little difference in baseline noise was observed by the addition of either acetone or toluene. This illustrates how APPI can be a complex process, dependant on analyte and mobile phase composition [6,9], photon energy [9], as well as specific source conditions (source geometry, lamp position, cone voltage, etc.). At the same time, for many of the normal phase solvents, APPI offers advantages over APCI in terms of source stability [20], avoiding deposit formation on the APCI corona needle and by the sensitivity enhancements afforded by careful selection of mobile phases and dopants.

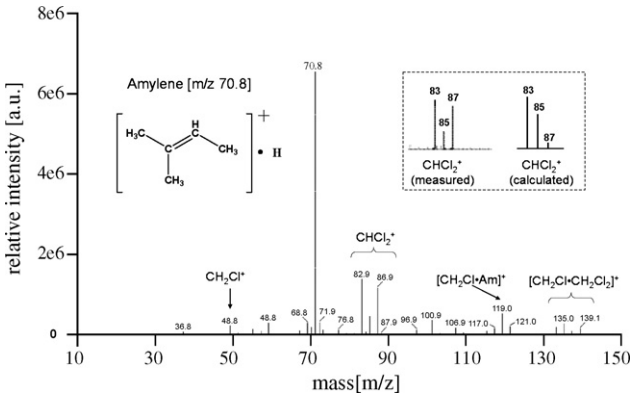

Fig. 5. Mass spectra of "pure" CH_2Cl_2 mobile phase (with 50–150 ppm amylene additive as a stabilizing agent). Insert mass spectra emphasize the isotopic distribution of the $CHCl_2^+$ mass peak, compared to the theoretical mass abundance values. Sample cone was set to a reduced value of 5 V to minimize fragmentation, with a small cone gas flow of 10 L/h to minimize entrance of neutral species within the z-spray chamber. Mass spectrum is average over 2 min of sampling.

3.6. The case of APPI with CH_2Cl_2

When "pure" CH_2Cl_2 is photoionized (Kr lamp at 10.0 eV and 10.6 eV), two features are apparent: (i) amylene $[M+H]^+$ ions from the common additive to CH_2Cl_2 (50–150 ppm or ca. 0.1 wt.%; IP = 8.69 eV) [21] and (ii) $CHCl_2^+$ ions, which must derive from CH_2Cl_2 despite its high IP of 11.32 eV (Fig. 5). We believe the source of the $CHCl_2^+$ ions is due to highly efficient photodissociation of CH_2Cl_2, generating Cl radical [22] (Cl^- is detected in significant amounts in negative ion mode), followed by the reaction of $CH_2Cl_2 + Cl \rightarrow CHCl_2 + HCl$. Based on the known reaction rate of $K_f = 9 \times 10^{-13}$ cm^3/mol s at 425 K [23], this reaction results in the rapid conversion of non-ionizable Cl radicals to ionizable $[CHCl_2]$ radicals (IP = 8.1 eV) [22] with a reaction half-life of $\tau = 1/(K_f[CH_2Cl_2])$, or 2 μs. Thus, not only are radicals being directly produced with sufficiently low IP to be ionized within the source, but also daughter products of photodissociation (primarily Cl radical) rapidly react away to result in additional ionizable radicals (primarily $CHCl_2$).

The isotope distribution of $CHCl_2^+$ in Fig. 5 deviates from the predicted distribution. The two lower isotopic abundances ($^{35}Cl^{35}Cl$ and $^{35}Cl^{37}Cl$) are relatively close to the predicted isotopic ratio; however, the *m/z* 87 signal is much greater than the calculated intensity for the $^{37}Cl^{37}Cl$ isotope. We conclude this is due to a contribution from another unknown ion since we are not aware of any photophysical isotope effect that could occur with such magnitude.

The effect of each mobile phase solvent component (i.e., pure individual solvent) on TAG sensitivity was evaluated using analytes SSS and LnLnLn. CH_2Cl_2 was found to generate analyte peak intensities comparable to those of iPrOH although the baseline noise level from CH_2Cl_2 is higher than that of iPrOH (results not shown). This is likely a result of the increase in background cations and their clusters when CH_2Cl_2 is used. It is also useful to note that addition of CH_3CN to pure CH_2Cl_2 (and indeed to other solvents presented in Table 2) results in a drop in signal intensity (until a dopant is added). This may be explained by the high proton affinity of CH_3CN (186 kcal/mol [24]) combined

with the high ionization potential of CH_3CN relative to the photon energies used (Fig. 4). This is in contrast to the addition of MeOH to CH_2Cl_2, resulting in a similar TAG response as obtained with dopants. In this case, although the proton affinity of MeOH is comparable to that of CH_3CN (180 kcal/mol) [24], direct photoionization of methanol dimers present in methanol vapor provides an alternative route for TAG ionization [9].

3.7. Limits of detection

Limits of detection for TAGs by LC–APPI-MS were determined by analyzing 10 μL of 1 ng/μL TAG standard mix in iPrOH in selected ion monitoring (SIM) mode using the conditions and LC gradient elution programs described in Fig. 3. The SIM was used for the most abundant ions for each TAG: $[M–RCOO]^+$ fragment ions for SSS, SSO and OOO and $[M+H]^+$ ions for LLO, LLL and LnLnLn (Fig. 2 and Table 1). The actual ions used for SIM analysis are as follows: LnLnLn: *m/z* 873.7 $[M+H]^+$; LLL: *m/z* 879.7 $[M+H]^+$; LLO: *m/z* 881.8 $[M+H]^+$; OOO: *m/z* 603.6 $[M+H–C18:1]^+$; SSO: *m/z* 605.7 $[M+H–C18:0]^+$; and SSS: *m/z* 607.6 $[M+H–C18:0]^+$.

For relative comparison, limits of detection (LODs at S/N = 3) for each analyte using a specific mobile phase were estimated from 10 ng injection using the ions indicated in Table 2. All six mobile phases gave comparable on-column LODs, estimated to be below 200 pg for most of the analytes tested here using the Waters ZQ. However, the particular solvent combinations of $MeOH/CH_2Cl_2$ and CH_3CN/CH_2Cl_2 resulted in LODs several times higher for SSS, a result of higher background noise associated with a CH_2Cl_2-based mobile phase (see above discussion).

3.8. Application of LC–APPI-MS to natural TAG oil

In order to illustrate the utility of APPI-MS combined with non-aqueous reversed phase chromatography, we present data for a natural tuna oil using a slow gradient of the CH_3CN/iPrOH mobile phase with acetone dopant on a Waters RX C_{18} column and Waters Micromass Q-Tof-1 mass spectrometer. The results are given in Figs. 6 and 7. Fig. 6(a) shows the total ion current (TIC) chromatogram for an acquired scan range of *m/z* 200–1400. The complexity of this TAG mixture is self-evident and the combination with mass spectrometry is essential for peak identification. As an example, consider the minor peaks I, II and III in the TIC trace given in Fig. 6(a). The background subtracted mass spectrum of peak II is shown in Fig. 7(a). Since tuna TAG oil is known to contain a high amount of polyunsaturated fatty acyl groups, the mass spectra would be expected to show abundant protonated molecules, as was seen for LnLnLn in Fig. 2. The TAG can be readily identified from the $[M+H]^+$ ion at *m/z* 997.9 as having fatty acyl groups totaling 64 carbons and 17 double bonds, which is most likely [20:5], [22:6] and [22:6] (i.e., EPA, DHA and DHA). Examination of the $[M–RCOO]^+$ fragment ion range shows two peaks at *m/z* 669.6, formed by loss of one molecule of DHA, and at *m/z* 695.6, formed by loss of one molecule of EPA. The greater abundance of *m/z* 669.6 than that of *m/z* 695.6 implies that the EPA is on the *sn*-2 position

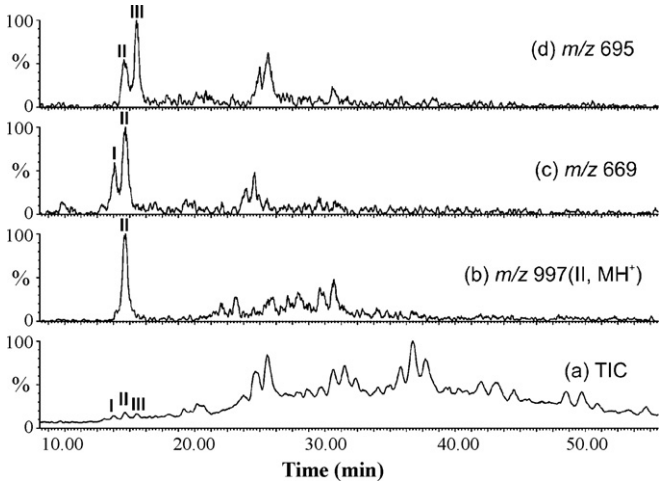

Fig. 6. LC–APPI-MS chromatograms of tuna oil using an acetonitrile/isopropanol gradient with acetone dopant.

which is typically lost less abundantly. The ion at *m/z* 1056.9 is presumed to be an adduct ion of the type $[M+iPrOH]^+$.

The mass chromatogram of *m/z* 669.6 (Fig. 6(c)) reveals that this ion containing EPA and DHA fatty acyl groups is also present in peak I. The mass spectrum of peak I (Fig. 7(b)) contains the $[M+H]^+$ ion at *m/z* 971.9 which would suggest two EPA and one DHA fatty acyl groups on the TAG. Examination of the $[M–RCOO]^+$ fragment ion region indicates DHA is on the *sn*-2 position by the low intensity of the fragment ion formed by loss of DHA.

The mass chromatogram of the fragment ion at *m/z* 695.6 containing two DHA moieties reveals (Fig. 6(d)) that this is a major ion in peak III. Indeed, the mass spectrum of peak III (Fig. 7(c)) contains this ion as the base peak and is the only significant fragment ion. The $[M+H]^+$ ion in the mass spectrum is at *m/z* 1023.9 which corresponds to the TAG containing three DHA fatty acyl groups, i.e., tridocosahexaenoin, consistent with the observation of only one type of $[M–RCOO]^+$ fragment ion containing two DHA chains.

The above discussion illustrates some of the potential offered by normal phase LC–APPI-MS in TAG analysis. Peaks I, II and

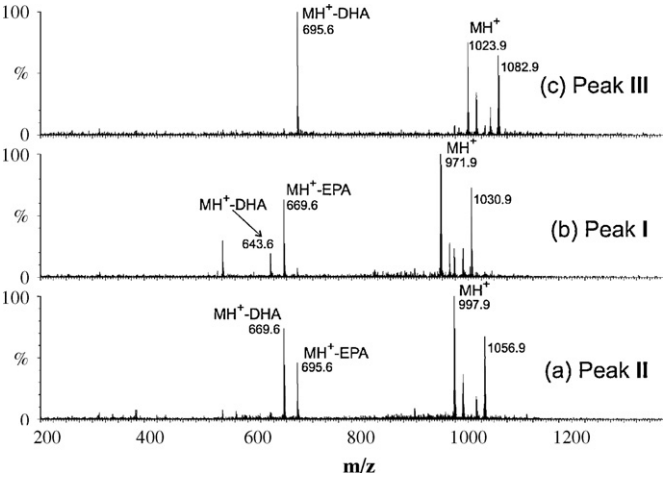

Fig. 7. APPI mass spectra extracted from peaks I–III from Fig. 6.

III are only minor components of the fish oil TAG (Fig. 6(a)) but nonetheless yield highly informative mass spectra.

4. Summary and conclusions

In this work, six binary mobile phases for non-aqueous reversed phase chromatography were tested for LC–APPI-MS analysis of six TAG model compounds. These analytes cover saturated and unsaturated TAGs with varying degree of unsaturation on their fatty acyl groups. With carefully adjusted gradient elution programs, all mobile phases selected offer comparable column separation performance on a C_{18} column. The analyte elution order on-column follows the same order of ECN of these compounds. CH_3CN/iPrOH is the preferred mobile phase since it results in low column backpressure, narrow peak widths and short retention times, and gives low odors during analysis.

APPI generates TAG mass spectra similar to those of APCI giving fragment ions $[M–RCOO]^+$ and/or protonated molecules $[M+H]^+$ as major ions. The intensity of $[M+H]^+$ increases as the degree of unsaturation increases. As with APCI spectra $[M–RCOO]^+$ fragment ion intensity can be related to the *sn*-2 substitution.

APPI sensitivity of TAG analytes varies greatly from one mobile phase to the other without dopants; however appropriate use of dopants brings peak area to comparable levels for all mobile phases (Table 2). The process of PCI is believed to be the dominant mechanism and hence either ionizable mobile phases (e.g., MeOH/iPrOH) or dopants (e.g., acetone) are required to achieve high sensitivity. High photoabsorption cross-sections of non-ionizable mobile phases may suppress APPI signals due to depletion of photons. All six mobile phases offer comparable overall on-column LODs, estimated to be below 200 pg for most of the analytes tested. These results indicate that LC–APPI-MS is a successful tool for neutral lipid analysis, giving high sensitivity using a wide variety of non-aqueous mobile phases. The analysis of tuna oil using the CH_3CN/iPrOH mobile phase with acetone dopant illustrates the application of these findings in complex TAG analysis.

Acknowledgements

We thank Dr. Karl A. Hanold (Syagen) for his help with instrument maintenance. This work is partially supported by the US National Institute of Health (SBIR Phase II, GM063430).

References

[1] F.B. Padley, F.D. Gunstone, J.L. Harwood, in: F.D. Gunstone, J.L. Harwood, F.B. Padley (Eds.), The Lipid Handbook Chapman and Hall, London, UK, 1994, p. 47.
[2] S.M. Grundy, in: E.E. Ziegler, L.J. Filer (Eds.), Present Knowledge in Nutrition, ILSI Press, Washington DC, USA, 1996, p. 44.
[3] J.L. Sebedio, New Trends in Lipid and Lipoprotein Analyses, AOCS Press, Champaign, Illinois, USA, 1995.
[4] W.R. Byrdwell, in: W.R. Byrdwell (Ed.), Modern Methods for Lipid Analysis by Liquid Chromatography/Mass Spectrometry and Related Techniques, AOCS Press, Champaign, IL, 2005, p. 298.
[5] S.-S. Cai, J.A. Syage, Anal. Chem. 78 (2006) 1191.
[6] S.-S. Cai, J.A. Syage, J. Chromatogr. A 1110 (2006) 15.
[7] D.B. Robb, T.R. Covey, A.P. Bruins, Anal. Chem. 72 (2000) 3653.
[8] T.J. Kauppila, T. Kuuranne, E.C. Meurer, M.N. Eberlin, T. Kotiaho, R. Kostiainen, Anal. Chem. 74 (2002) 5470.
[9] L.C. Short, S.-S. Cai, J.A. Syage, J. Am. Soc. Mass Spectrom. 18 (2007) 589.
[10] L.C. Short, K.A. Hanold, S.-S. Cai, J.A. Syage, Rapid Commun. Mass Spectrom. 21 (2007) 1561.
[11] H.R. Mottram, in: W.R. Byrdwell (Ed.), Modern Methods for Lipid Analysis by Liquid Chromatography/Mass Spectrometry and Related Techniques, AOCS Press, Champaign, IL, 2005, p. 276.
[12] M. Buchgraber, F. Ulberth, H. Emons, E. Anklam, Eur. J. Lipid Sci. Technol. 106 (2004) 621.
[13] P. Kalo, A. Kemppinen, V. Ollilainen, A. Kuksis, Int. J. Mass Spectrom. 229 (2003) 167.
[14] P. Dugo, T. Kumm, M.L. Crupi, A. Cotroneo, L. Mondello, J. Chromatogr. A 1112 (2006) 269.
[15] P. Dugo, T. Kumm, M.L. Presti, B. Chiofalo, E. Salimei, A. Fazio, A. Cotroneo, L. Mondello, J. Sep. Sci. 28 (2005) 1023.
[16] L. Mondello, P.Q. Tranchida, V. Stanek, P. Jandera, G. Dugo, P. Dugo, J. Chromatogr. A 1086 (2005).
[17] K.A. Hanold, S.M. Fischer, P.H. Cormia, C.E. Miller, J.A. Syage, Anal. Chem. 76 (2004) 2842.
[18] S.T. Tsai, J.C. Jiang, Y.T. Lee, A.H. Kung, S.H. Lin, C.K. Ni, J. Chem. Phys. 111 (1999) 3434.
[19] J.A. Syage, J. Am. Soc. Mass Spectrom. 15 (2004) 1521.
[20] S.-S. Cai, K.A. Hanold, J.A. Syage, Anal. Chem. 79 (2007) 2491.
[21] J.C. Traeger, J. Phys. Chem. 90 (1986) 4114.
[22] S.Y. Chiang, M. Bahou, K. Sankaran, Y.P. Lee, H.F. Lu, M.D. Su, J. Chem. Phys. 118 (2003) 62.
[23] M.G. Bryukov, I.R. Slagle, V.D. Knyazev, J. Phys. Chem. A 106 (2002) 10532.
[24] E.P. Hunter, S.G. Lias, J. Phys. Chem. Ref. Data 27 (1998) 413.